

Synthesis, Structural Investigation, Hirshfeld Surface Analysis, and Biological Evaluation of *N*-(3-Cyanothiophen-2-yl)-2-(thiophen-2-yl)acetamide

Şükriye Çakmak, Sevgi Kansız,* Mohammad Azam,* Cem Cüneyt Ersanlı, Önder İdil, Aysel Veyisoğlu, Hasan Yakan, Halil Kütük, and Arunabharam Chutia



Cite This: *ACS Omega* 2022, 7, 11320–11329



Read Online

ACCESS |



Metrics & More

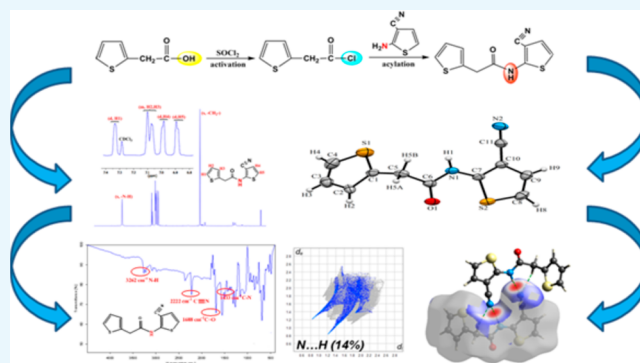


Article Recommendations



Supporting Information

ABSTRACT: In this study, a novel heterocyclic amide derivative, *N*-(3-cyanothiophen-2-yl)-2-(thiophen-2-yl)acetamide (**I**), was obtained by reacting 2-aminothiophene-3-carbonitrile with activated 2-(thiophen-2-yl)acetic acid in a *N*-acylation reaction and characterized by elemental analyses, FT-IR, ^1H and ^{13}C NMR spectroscopic studies, and single crystal X-ray crystallography. The crystal packing of **I** is stabilized by C–H \cdots N and N–H \cdots N hydrogen bonds. In addition, **I** was investigated computationally using the density functional theory (DFT) method with the B3LYP exchange and correlation functions in conjunction with the 6311++G(d,p) basis set in the gas phase. Fukui function (FF) analysis was also carried out. Electrophilicity-based charge transfer (ECT) method and charge transfer (ΔN) were computed to examine the interactions between **I** and DNA bases (such as guanine, thymine, adenine, and cytosine). The most important contributions to the Hirshfeld surface are H \cdots H (21%), C \cdots H (20%), S \cdots H (19%), N \cdots H (14%), and O \cdots H (12%). An ABTS antioxidant assay was used to evaluate the *in vitro* antioxidant activity of **I**. The compound exhibited moderate antioxidant activity. The antimicrobial activity of the title molecule was investigated under aseptic conditions, using the microdilution method, against Gram-positive and Gram-negative bacterial strains, and it also demonstrated significant activity against yeasts (*Candida glabrata* ATCC 90030, *Candida krusei* ATCC 34135). The findings revealed that the molecule possesses significant antioxidant and antimicrobial properties.



INTRODUCTION

In organic chemistry, amides that contain the R–CO–NHR functional group are typically formed when a carboxylic acid reacts with an amine.^{1,2} Furthermore, the amide bond exists in the structures of proteins, peptides, and other important biological molecules.³ It is also an important functional group and essential component of many pharmaceuticals, natural products, agrochemicals, and polymers.^{4,5} Recently, the chemistry of amide compounds has recently been a fascinating field of research. Some of these compounds have been shown to have significant antifungal, antibacterial,^{6,7} antioxidant,^{7–11} insecticide,¹² anticonvulsant, analgesic, antitumor, anti-inflammatory, and anti-HSV activity.^{13–17} Additionally, amides also have a broad range of different applications in polymers, dyes, and liquid crystals.^{6,9,17}

Herein, we designed a novel amide compound containing a heteroatom and synthesized by *N*-acylation of 2-aminothiophene-3-carbonitrile with activated 2-(thiophen-2-yl)acetic acid. The structure of **I** was confirmed by IR, ^1H NMR, ^{13}C NMR, elemental analysis, and X-ray diffraction. The ABTS antioxidant assay was used to measure *in vitro* antioxidant

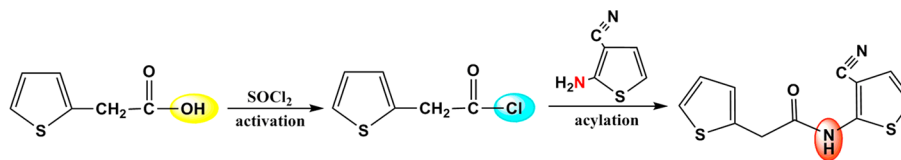
activity. In addition, the antimicrobial activity of **I** *in vitro* was also performed to test its antimicrobial effects against various microbial species. In recent years, the direct comparison of experimental and theoretical results for the characterization of a compound has been of great importance.^{18,19} Therefore, in this study, we applied density functional theory (DFT) to understand the detailed electronic properties of **I** at the B3LYP/6-311++G(d,p) level of theory. Fukui function for electrophilic $f_k^+(r)$ and nucleophilic attack $f_k^-(r)$ were used to assess the chemical reactivity. Electron affinity (EA), ionization potential (IA), hardness (η), and chemical potential (μ) were also investigated. Finally, the geometry optimizations were obtained in the same level of theory to analyze the interactions

Received: January 20, 2022

Accepted: March 7, 2022

Published: March 21, 2022



Scheme 1. Synthesis of *N*-(3-Cyanothiophen-2-yl)-2-(thiophen-2-yl)acetamide

between compound **I** and the DNA bases (such as guanine, thymine, adenine, and cytosine). The single point energy of the optimized structure was computed for its neutral, cation, and anion states to understand the electrophilicity-based charge transfer (ECT) method and charge transfer (ΔN) phenomena. Hirshfeld surface analysis was used to specify the close intermolecular interactions in the molecule.

EXPERIMENTAL PART

Instruments. Reagents have been bought from Sigma-Aldrich, Merck, or ABCR, and solvents used are of analytical purity. ^1H and ^{13}C NMR spectra were taken on Bruker/Biospin (400 MHz) in CDCl_3 spectrometer. FT-IR spectrum was recorded on a Bruker Vertex 80 V spectrophotometer. Melting points were recorded with a Stuart SMP 30. Elemental analyses were performed with a Costech, ECS 4010 elemental analyzer.

Synthesis of *N*-(3-Cyanothiophen-2-yl)-2-(thiophen-2-yl)acetamide, **I, $\text{C}_{11}\text{H}_8\text{N}_2\text{OS}_2$.** Synthesis of *N*-(3-cyanothiophen-2-yl)-2-(thiophen-2-yl)acetamide is a two-step process. In this two-step process, 2-(thiophen-2-yl)acetic acid was first activated by converting it into 2-(thiophen-2-yl)acetyl chloride and then reacted with 2-aminothiophene-3-carbonitrile. We have described the activation of the first step, carboxylic acid, with thionyl chloride in our previous study.²⁰ The acylation step was carried out in the second step, which involved dissolving 2-aminothiophene-3-carbonitrile (10 mmol) in 12 mL of THF and the addition of 0.95 mL of triethylamine (10 mmol) into it. 2-(Thiophen-2-yl)acetyl chloride (1.19 g, 11 mmol) dissolved in 10 mL of THF was slowly added to this reaction mixture. After 15 h of stirring at room temperature, the reaction mixture was filtered and the white salt residue was removed. The solid product was washed with water several times before being filtered, dried, and crystallized from acetonitrile.

Yield: 1.68 g, mp 163–166 °C, yield 58%; Anal. Calcd for $\text{C}_{11}\text{H}_8\text{N}_2\text{S}_2\text{O}$: C, 53.17; H, 3.22; N, 11.28; S, 25.78. Found: C, 53.19; H, 3.20; N, 11.06; S, 24.20.²¹

The *N*-(3-cyanothiophen-2-yl)-2-(thiophen-2-yl)acetamide molecule was synthesized through a two-step reaction shown in Scheme 1. The acid chloride intermediate was formed in the first step, activation, and then the key intermediates reacted with the heterocyclamine in the second step. We preferred the amide synthesis method from acyl chlorides, which are widely used in the literature. Due to this method, we were able to easily separate the product from the reaction medium.

Crystal Structure Determination. A Bruker diffractometer equipped with graphite-monochromatic Mo $K\alpha$ radiation at 296 K ($\lambda = 0.71073 \text{ \AA}$) was used to collect the data of **I**. A Bruker APEX2²² was used during the data collection. The structure of the cobalt complex was solved using SHELXT,²³ and refinement was made on Olex2 with SHELXL-2018 with least-squares minimization versus F^2 .²⁴ Also, Mercury for Windows,²⁵ PLATON,²⁶ WinGX,²⁷ and publCIF²⁸ were used

for the process. Table 1 summarizes the experimental details for **I**.

Table 1. Data Collection and Structure Refinement for **I**

CCDC	2132193
chemical formula	$\text{C}_{11}\text{H}_8\text{N}_2\text{OS}_2$
temperature (K)	296
space group	$P2_1/c$
crystal system	monoclinic
M_r	448.31
a, b, c (Å)	4.4439 (2), 22.6851 (13), 11.1242 (7)
α, β, γ (deg)	90, 96.530 (2), 90
volume, V (Å ³)	1114.16 (11)
crystal size (mm)	0.30 × 0.25 × 0.22
calculated density (Mg/m ³)	1.480
F_{000}	512
μ (mm ⁻¹)	0.46
Z	4
diffractometer	Bruker APEX3 CCD
θ range (deg)	$2.6 \leq \theta \leq 27.3$
wavelength (Å)	0.71073
measurement method	ω scan
absorption correction	Multiscan
$h_{\text{min}}, h_{\text{max}}$	−5, 5
$k_{\text{min}}, k_{\text{max}}$	−30, 30
$l_{\text{min}}, l_{\text{max}}$	−14, 14
R_{int}	0.046
reflections collected	31325
independent reflections	2751
observed reflections [$I > 2\sigma(I)$]	1966
refinement method	SHELXL18/3
parameters	148
$R[F^2 > 2\sigma(F^2)]$	0.060
$wR(F^2)$	0.204
Goof = S	1.06
$\Delta\rho_{\text{min}}, \Delta\rho_{\text{max}}$ (e/Å ³)	−0.48, 0.84

Computational Details. Gaussian 09W²⁹ package was used to fully relax all the geometries (Figure 1b) at the B3LYP/6-311++G(d,p) level of theory,^{30,31} which is considered to be an effective and low-cost approach to obtain reliable molecular structures and for the analyses of Fukui functions. To confirm the local minima of the studied systems, vibrational frequency calculations were also performed. The *CrystalExplorer21* program³² was used to analyze the Hirshfeld surfaces.

Antioxidant Activity Using ABTS Radical Scavenging Assay. ABTS radical cation decolorization assay was performed for free radical scavenging activity of **I**. ABTS^{•+} cation radical was generated by reacting 7 mM ABTS in water with 2.45 mM potassium persulfate (1:1) and leaving it at room temperature in the dark for 12–16 h before use. ABTS^{•+} solution was solubilized with methanol and then an absorbance of 0.700 at 734 nm was obtained. A serial solubilization of 0.5–0.0078 mM concentration of **I** was mixed with ABTS^{•+}

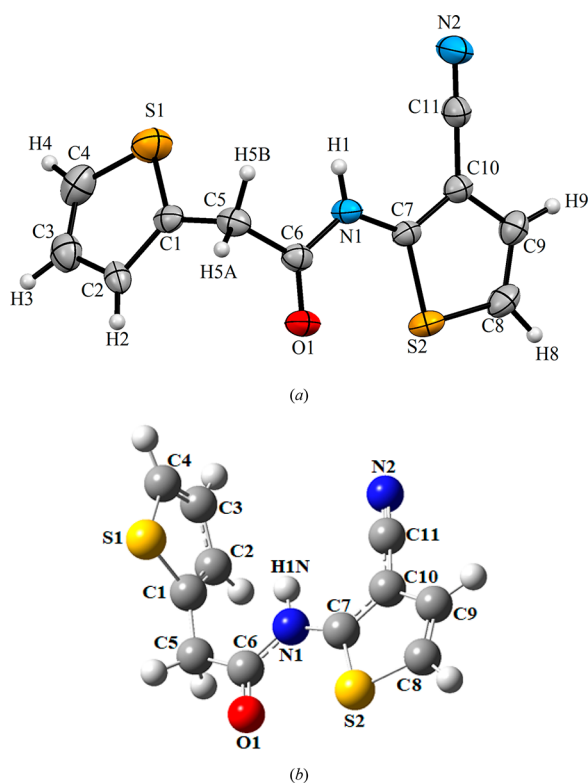


Figure 1. (a) Crystal structure and (b) optimized geometry of I.

solution, and absorbance was measured 30 min after first stirring. Percent inhibition of absorbance at 734 nm was computed using the following formula:

$$\text{ABTS}^{\bullet} + \text{scavenging effect (\%)} \\ = ((AB - AA)/AB) \times 100$$

Here, AB stands for the absorbance of ABTS radical + methanol; AA represents the absorbance of ABTS radical + sample extract/standard.

Antimicrobial Activity. Minimal Inhibitory Concentration (MIC) Method. Antimicrobial activities were applied against standard Gram-positive bacterial strains (*Staphylococcus aureus* ATCC 6538P, *Listeria monocytogenes* ATCC 19111, *Micrococcus luteus* NRRL B-4375) and gram strain negative (*Escherichia coli* ATCC 25922, *Klebsiella pneumoniae* ATCC 700603, *Salmonella typhimurium* ATCC 14028), yeasts (*Candida glabrata* ATCC 90030, *Candida krusei* ATCC 34135) using the Minimal Inhibitory Concentration Method (MIC). The title molecule used in this study was dissolved in dimethyl sulfoxide (DMSO) at a suitable concentration. To

incubate all cultures, they were maintained in broth at 37 °C for 24 h. Then, 50 mL nutrient broth was used to suspend the bacterial and yeast cells. The turbidity of bacterial and yeast suspensions was adjusted to a concentration of nearly 10⁶ cells/mL by pairing with 0.5 McFarland turbidity standards. Microorganisms were transferred as 1 mL aliquots into test tubes and added to mixtures. The incubation time of all test cultures is 24 h in an incubator at 37 °C. The MIC value (μg/mL) (Table 2) was used for the minimum inhibitory concentration at which no growth was observed.

RESULTS AND DISCUSSION

Crystal Structure of I, C₁₁H₈N₂OS₂. The title compound (Figure 1a), *N*-(3-cyanothiophen-2-yl)-2-(thiophen-2-yl)acetamide (I), is a heterocyclic amide derivative formed from 2-aminothiophene-3-carbonitrile with activated 2-(thiophen-2-yl)acetic acid in a *N*-acylation reaction. The crystal structure of I crystallized in a monoclinic space group *P*₂₁/*c*, and *Z* = 4 (Table 1). There is one independent molecule in the asymmetric unit. The dihedral angle causing the molecule to be nonplanar between thiophene and thiophene-3-carbonitrile ring is 74.27(10)° dihedral angle. The thiophene ring (C1–C4/S1) and the C1/C5/C6/N1/C7 acetamide bridge are twisted with a dihedral angle of 60.38(22)°. The angle between the planes of the C1/C5/C6/N1/C7 acetamide bridge and the thiophene-3-carbonitrile ring is 75.70(25)°. The molecules are linked by C–H⋯N and N–H⋯N hydrogen bonds in the crystal (Table 3). The N1 and C5 atoms act as hydrogen-bond donors, via atoms H1 and H5B, to atom N2 in the molecule at (−*x*, 1 − *y*, 1 − *z*), forming centrosymmetric *R*₂²(12) and *R*₂²(16) rings centered at (0, 1/2, 1/2). The combination of these hydrogen bonds produces the *R*₂¹(6) ring (Figure 2). The nitrile group is typical of the C11≡N2 triple bond [1.142(5) Å], while the C6–O1 bond distance shows a typical double bond character at 1.217(4) Å (Table 4). The S1–C1, S1–C4, S2–C7, and S2–C8 bond lengths are 1.702(3), 1.688(5), 1.723(3), and 1.718(4) Å, which are within the range of values in the previously reported thiophene ring-containing compounds.^{33–35}

IR Spectroscopy. Figure 3 shows the experimental IR spectrum of I. The absorption band at around 3262 cm^{−1} shows the existence of N–H stretching vibration. The characteristic absorption C=O (amide I) band of the amide compound appeared at 1688 cm^{−1}, whereas another band was observed ~1433 cm^{−1} corresponding to the C–N stretching vibration with the N–H bending vibration (amide II). The other significant band appearing at 2222 cm^{−1} belongs to the C≡N stretching vibration. These experimental data support the structure of similar molecules in the literature.^{36–42}

Table 2. Minimum Inhibition Concentrations (MIC's) of the Tested Compound

	Gram-negative bacteria (μg/ml)			Gram-positive bacteria (μg/ml)			Yeast (μg/ml)	
<i>Escherichia coli</i> ATCC 25922	<i>Salmonella typhimurium</i> ATCC 14028	<i>Klebsiella pneumoniae</i> ATCC 700603	<i>Listeria monocytogenes</i> ATCC 19111	<i>Micrococcus luteus</i> NRRL B-4375	<i>Staphylococcus aureus</i> ATCC 25923	<i>Candida glabrata</i> ATCC 90030	<i>Candida krusei</i> ATCC 34135	
	1000	2000	2000	125	250	250	2000	2000
DMSO	>4000	>4000	>4000	>4000	>4000	>4000	>4000	>4000

Table 3. Hydrogen Bonds of I (Å, deg)

D–H...A	D–H	H...A	D...A	D–H...A	symmetry code
N1–H1...N2 ⁱ	0.84(2)	2.21(2)	3.049(4)	172(4)	(i) $-x, -y + 1, -z + 1$
C5–H5B...N2 ⁱ	0.97	2.57	3.409(5)	145	

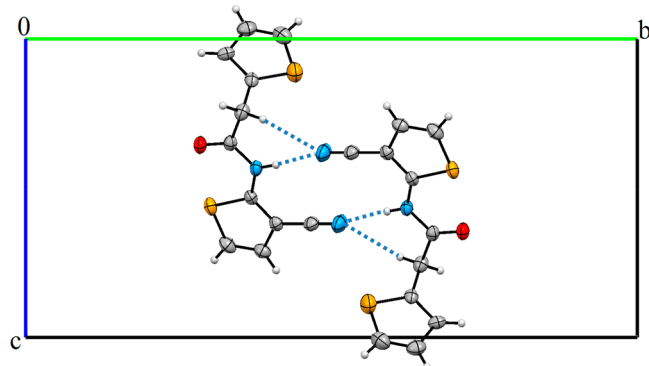
Figure 2. View of crystal packing of I forming $R_2^1(6)$, $R_2^2(12)$, and $R_2^2(16)$ rings.

Table 4. Some Geometric Parameters of I (Å, deg)

geometric parameters	X-ray	geometric parameters	X-ray
bond lengths (Å)		bond angles (deg)	
C1–S1	1.702 (3)	C1–S1–C4	92.5 (2)
C4–S1	1.688 (5)	C7–S2–C8	91.61 (17)
C7–S2	1.723 (3)	C6–N1–C7	124.2 (3)
C8–S2	1.718 (4)	N1–C6–O1	121.4 (3)
C6–O1	1.217 (4)	C5–C6–O1	122.8 (3)
C11–N2	1.142 (5)	C7–C10–C11	122.7 (3)
C9–C10	1.429 (5)	C9–C10–C11	124.4 (3)
C6–N1	1.370 (4)	torsion angles (deg)	
C7–N1	1.380 (4)	S2–C7–C10–C11	−177.6 (3)
C10–C11	1.421 (5)	S1–C1–C5–C6	−92.7 (3)
C1–C5	1.504 (5)	N1–C7–C10–C9	179.7 (3)
C5–C6	1.511 (5)	C1–C5–C6–O1	−79.8 (4)

NMR Spectroscopy. The ¹H NMR spectrum of I was taken in CDCl₃ (Figure 4). The singlet signal at 9.32 ppm (s, 1H, NH–C=O) was attributed to the amide group proton in the structure, while the signal at 4.10 ppm (s, 2H, –CH₂–) belongs to methylene protons. The signals of the thiophene ring protons H1, H2, and H3 were observed in the region of $\delta = 7.06$ –7.33 ppm as a multiplet, excepting the H1 proton, observed at 7.33 ppm as a doublet. The other thiophene ring protons H4 and H5 interacted with each other and appeared as doublets at 6.98 and 6.89 ppm, respectively.

Figure 5 shows the ¹³C NMR spectrum of I taken in CDCl₃. The ¹³C NMR spectrum of the title molecule displayed 11 different resonances compatible with the proposed structure. Eight aromatic carbons are belonging to two thiophene rings. The C5 and C4 carbons which gave the signal at 149.6 and 134.0 ppm, respectively, were the most downfield in comparison with the other carbons of the thiophene rings. The other thiophene ring carbons appeared at 28.02–93.04 ppm.

The signal for the methylene group (–CH₂) between the carbonyl group and the thiophene ring was observed at 36.82 ppm while the signal at 167.16 ppm was assigned to the amide carbonyl group. The presence of the acetoxy group on the

phenyl ring causes the carbon of the nitrile group to shift to the lower domain. The nitrile group (–C≡N) carbon attached to the thiophene ring was observed at 114.45 ppm. The nitrile group (–C≡N) (C6) on the thiophene ring was observed at 114.45 ppm.

Consequently, these experimental data also support the structure of the title compound and previously reported values for similar structures.^{39–42}

Fukui Function Analysis. The Fukui function (FF) provides information about the local reactivity of the whole molecule and is one of the most commonly used determinants of local reactivity.^{43,44} The nucleophilic, electrophilic, and radically prone positions in I were assessed with FF. The compact Fukui functions⁴⁵ are represented as $f_k^+(\mathbf{r})$ for the nucleophilic attack, $f_k^-(\mathbf{r})$ for an electrophilic attack, and $f_k^0(\mathbf{r})$ for a free radical attack.

$$f_k^-(\mathbf{r}) = q_k(\mathbf{r})(N) - q_k(\mathbf{r})(N - 1) \quad (1)$$

$$f_k^+(\mathbf{r}) = q_k(\mathbf{r})(N + 1) - q_k(\mathbf{r})(N) \quad (2)$$

$$f_k^0(\mathbf{r}) = \frac{1}{2}[q_k(\mathbf{r})(N + 1) - q_k(\mathbf{r})(N - 1)] \quad (3)$$

The difference between nucleophilic and electrophilic FF is defined as the binary identifier [$\Delta f_k(\mathbf{r})$] given below:

$$\Delta f_k(\mathbf{r}) = [f_k^+(\mathbf{r}) - f_k^-(\mathbf{r})] \quad (4)$$

If $\Delta f_k(\mathbf{r}) > 0$, the region is preferred for a nucleophilic attack, whereas if $\Delta f_k(\mathbf{r}) < 0$, the site is preferred for an electrophilic attack. The binary identifiers with their sign provide a clear distinction between the nucleophilic and electrophilic attack in a given region by providing a positive value for the region susceptible to nucleophilic attack and a negative value for the electrophilic attack. The binary identifier condition shows that the nucleophilic region for I involves C1, C3, C4, C8, C9, and C10 (positive value, i.e., $\Delta f_k(\mathbf{r}) > 0$) atoms [Table 5]. Similarly, the electrophilic regions are found on C2, C5, C6, C7, C11, O1, N1, N2, S1, and S2 atoms (negative value, i.e., $\Delta f_k(\mathbf{r}) < 0$). The results of FF show that compound I was more prone to electrophilic attack than nucleophilic attack and radical attack.

Electrophilicity-Based Charge Transfer (ECT) Method.

The ECT calculation is applied to determine the direction of charge transfer. The ECT method is of great importance to search for molecules and DNA bases that are electron acceptors or donors (electrophilic or nucleophilic behavior). In the case where ECT is greater than zero, charges are transferred from the base to the functional group, while if ECT is less than zero, charges migrate from the functional group to the base compound.⁴⁶ The electron affinity (EA) and ionization potential (IP) obtained from the energy of anionic, cationic, and neutral types are expressed as given below.

$$IP = [E(N - 1) - E(N)] \quad (5)$$

$$EA = [E(N) - E(N + 1)] \quad (6)$$

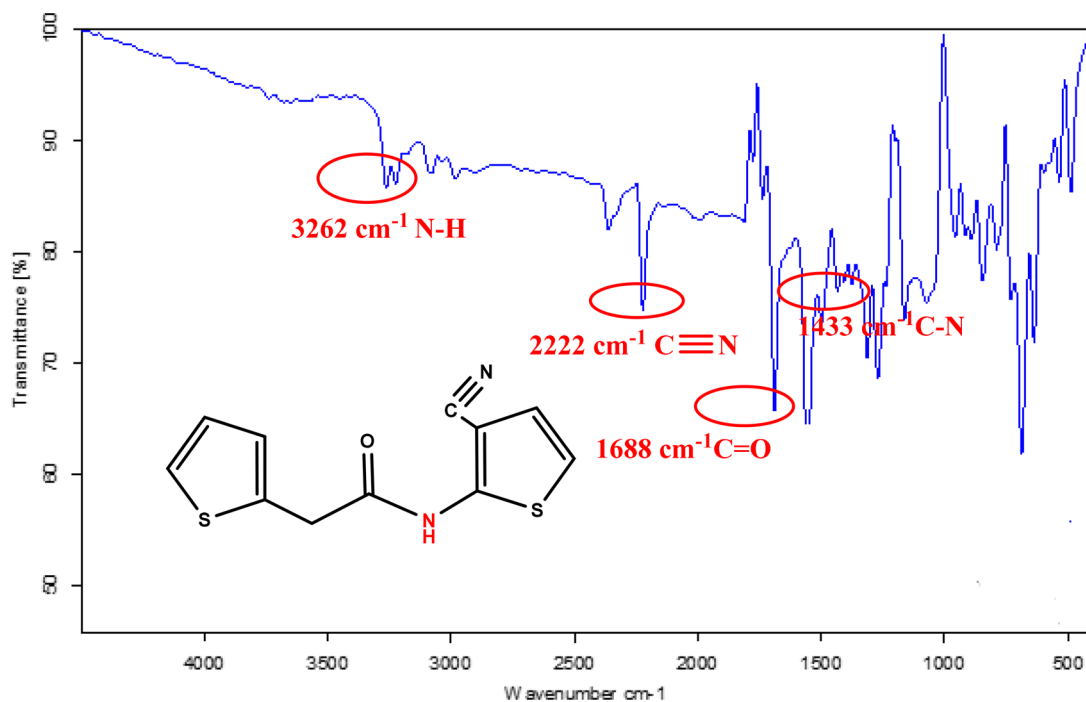


Figure 3. IR spectrum of *N*-(3-cyanothiophen-2-yl)-2-(thiophen-2-yl) acetamide.

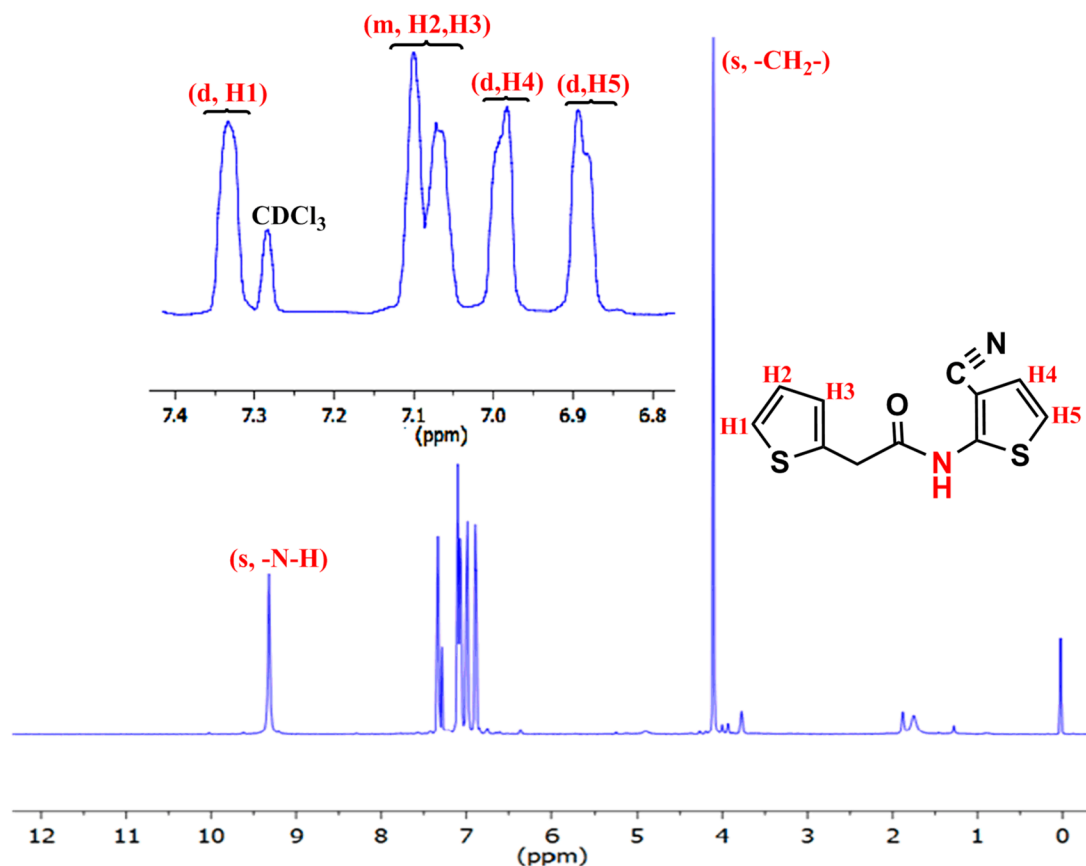


Figure 4. ^1H NMR spectrum of *I*.

The stabilization value in energy is measured with the new reactivity index when the system reserves the additional electronic load (ΔN). The electronic chemical potential of the molecule is effective in determining the direction of charge transfer. After an electrophile receives an electronic charge, its

energy decreases, and thus the electronic chemical potential becomes negative. The species may behave like a nucleophile with a lower electrophilic index in a reaction between two molecules. From the electrophilicity index results, it appears that DNA-bases such as cytosine, adenine, thymine, and

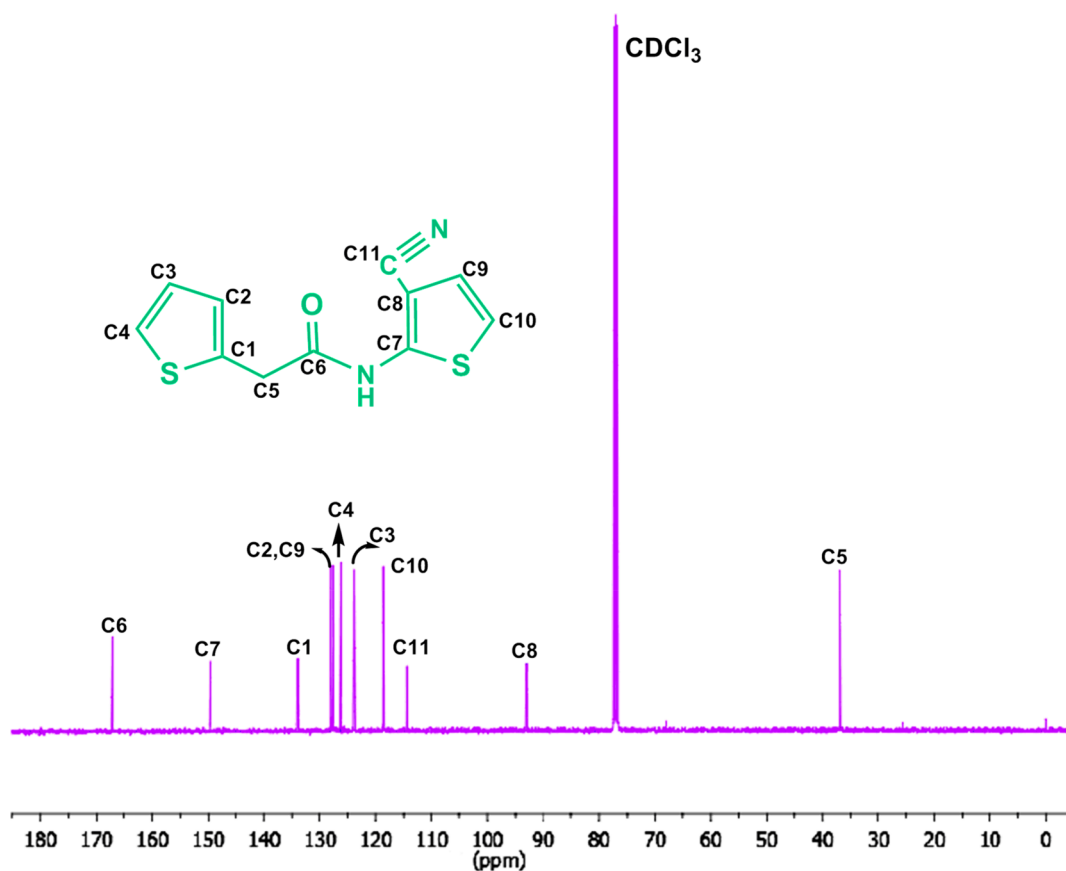


Figure 5. ^{13}C NMR spectrum of I.

Table 5. Results of the Natural Population Analysis (NPA) for I

atom	q_k^0	q_k^+	q_k^-	f_k^-	f_k^+
C1	-0.23911	-0.19579	-0.25123	0.01212	0.04332
C2	-0.25265	-0.24466	-0.30465	0.05200	0.00799
C3	-0.24474	-0.19263	-0.25004	0.00530	0.05211
C4	-0.37493	-0.30184	-0.42038	0.04545	0.07309
C5	-0.49603	-0.51053	-0.49164	-0.00439	-0.01450
C6	0.69587	0.70071	0.61084	0.08503	0.00484
C7	0.05599	0.11139	-0.02532	0.08131	0.05540
C8	-0.39458	-0.25352	-0.46233	0.06775	0.14106
C9	-0.20415	-0.17736	-0.21147	0.00732	0.02679
C10	-0.27316	-0.17606	-0.33920	0.06604	0.09710
C11	0.28127	0.24577	0.27757	0.00370	-0.03550
O1	-0.60117	-0.52799	-0.67673	0.07556	0.07318
N1	-0.62357	-0.55701	-0.54771	0.07586	0.06656
N2	-0.32644	-0.20934	-0.44469	0.11825	0.1171
S1	0.43262	0.48268	0.37975	0.05287	0.05006
S2	0.50290	0.56078	0.38703	0.11587	0.05788

guanine are good enough nucleophiles to attack $\text{C}_{11}\text{H}_8\text{N}_2\text{OS}_2$ (I). ECT is the difference between ΔN_{max} values of interacting molecules. Two molecules, A (I) and B (guanine, cytosine, thymine, and adenine) can be considered to be approaching each other; here, two situations arise: (i) $\text{ECT} < 0$, charge flow from A to B, and (ii) $\text{ECT} > 0$, charge flow from B to A. ECT is computed with the following expressions:

$$\text{ECT} = (\Delta N_{\text{max}})_A - (\Delta N_{\text{max}})_B \quad (7)$$

$$(\Delta N_{\text{max}})_A = \mu_A/\eta_A \text{ and } (\Delta N_{\text{max}})_B = \mu_B/\eta_B \quad (8)$$

where μ_A , μ_B and η_A , η_B are the chemical potentials and chemical hardness of systems A and B, respectively.⁴⁷ The ECT values for the guanine, adenine, thymine, and cytosine, were obtained as 0.11589, 0.07436, 0.05139, and -0.49282, respectively. In Table 6 are summarized the IP, EA, μ , η , ΔN_{max} and ECT values for I and DNA bases. From these results, it is seen that electrons were transfused from the DNA bases (guanine, adenine, and cytosine) to I. Here, the cytosine, adenine, and guanine bases are the electron donor, while I is an electron acceptor. In addition, while the DNA bases of adenine, cytosine, and guanine showed nucleophilic nature, I exhibited an electrophilic nature. According to the ECT results, it is seen that I interacts more with thymine than other DNA bases. Also, only the thymine base is treated as the electron acceptor.

Hirshfeld Surface Analysis. Using Hirshfeld surface (HS) analysis and fingerprint plots (FPs) are frequently used methods to analyze the contribution and percentage of distinct intermolecular interactions to the crystal packing.^{48,49} This method has received special attention in recent years, as it allows an accurate and complete understanding of intermolecular interactions.^{50–56} The Hirshfeld surface is defined as based on the normalized contact distance (d_{norm}) given by eq 9. To recognize the interatomic contacts, a red, blue, and white color scheme is used, representing the Hirshfeld surface calculated from the d_{norm} . In here, while a red spot shows the shortest contacts, the blue spot shows longer contacts.

Table 6. IP, EA, μ , η , ΔN_{max} and ECT values for I

compound and DNA bases	IP (au)	EA (au)	μ (au)	η (au)	ΔN_{max}
I (C ₁₁ H ₈ N ₂ O ₅)	5.4×10^{-3}	0.2989	-0.15215	-0.14675	1.03670
adenine	-0.01258	0.30519	-0.14630	-0.158886	0.92081
ECT = 0.11589					
cytosine	-0.00616	0.321254	-0.15754	-0.163709	0.96234
ECT = 0.07436					
guanine	-0.00214	0.290467	-0.14415	-0.146308	0.98531
ECT = 0.05139					
thymine	0.076022	0.3631556	-0.21958	-0.143566	1.52952
ECT = -0.49282					

$$d_{norm} = \frac{d_i - d_i^{rdw}}{d_i^{rdw}} + \frac{d_e - d_e^{rdw}}{d_e^{rdw}} \quad (9)$$

Figure 6 illustrates the Hirshfeld surface mapped with d_{norm} , d_i , d_e shape index, and curvedness; the indexes are -0.4512 to

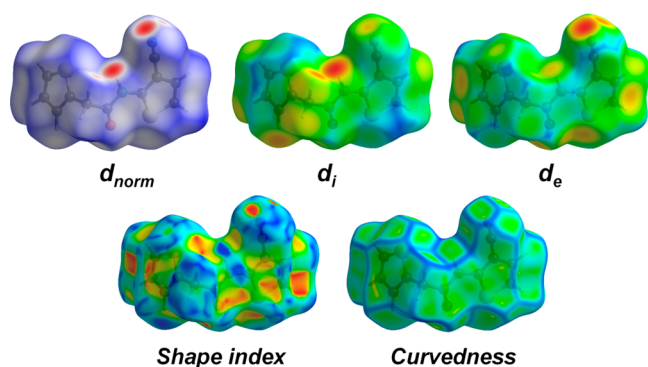


Figure 6. Hirshfeld surface mapped with d_{norm} , d_i , d_e shape index, and curvedness of I.

1.0427, 0.8369 to 2.5676, 0.8346 to 2.5514, -1 to 1, and -4 to 4 Å for I, respectively. Figure 7 shows the important interactions visible on the HSs as well as in the 2D fingerprints. H...H, C...H/H...C, S...H/H...S, N...H/H...N, and O...H/H...O interactions exist in the fingerprint plots of I. With a value of 21%, the contribution of H...H interactions has the largest share in the crystal packing of I. N...H/H...N interactions have a smaller share with a 14% contribution, while the heteronuclear interactions appear as in two long sharp. O...H interactions are related to C5-H5B...N2ⁱ and N1-H1...N2ⁱ intermolecular hydrogen bonds. S...H/H...S (19%) and C...H/H...C (20%) interactions form with two broad short spikes (Figure 7). The full intermolecular interactions and their percentages in I are shown in Figure 8. The HS and its 2D-FP are very useful tools to get information about the contributions of various intermolecular interactions that provide the stabilizing the molecular structure.

Evaluation of Antioxidant Activity. Antioxidants can avoid oxidation of oxidizable substrates when they exist in lower concentrations than the substrate.⁵⁷ Therefore, the discovery of substances with antioxidant properties has become important for human health. In here, the antioxidant activity of the newly prepared title molecule has been investigated to evaluate the radical scavenging activity of I according to the ABTS assay. Figure 9 gives the results of the ABTS radical scavenging activity. Various concentrations of (0.5–0.0078 mM) compound were mixed, and ABTS radical and dose-dependent radical scavenging activities were observed. The

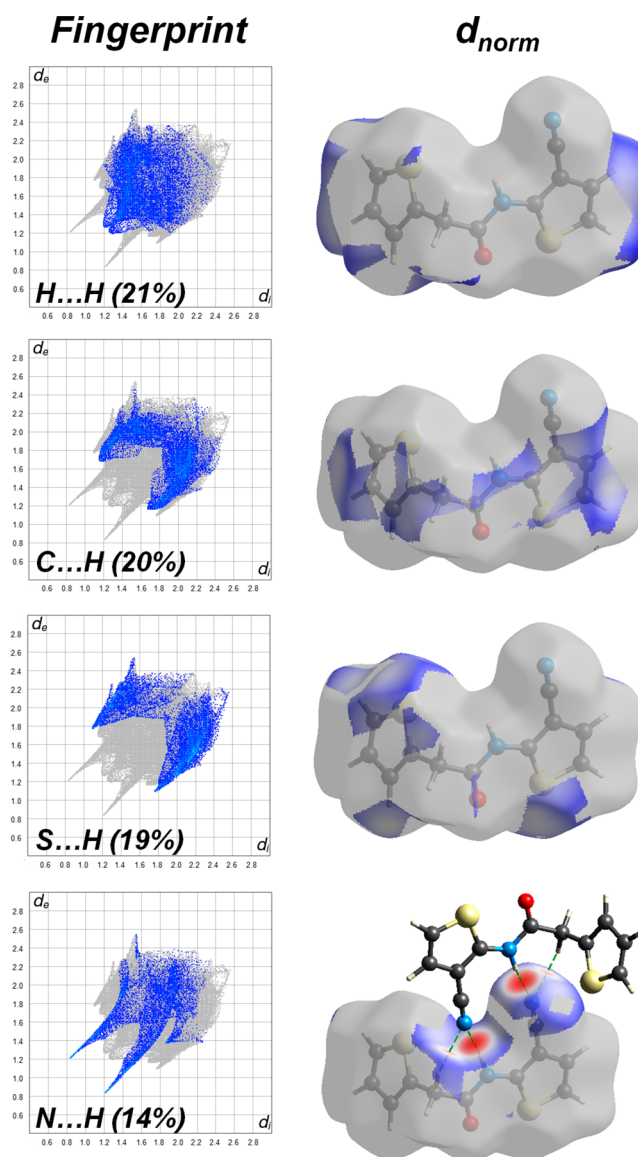


Figure 7. Two-dimensional fingerprint plots and HS for I.

IC50 value of the compound and BHA were calculated as 0.18 mM and 0.019 mg/mL, respectively. As a result, it has been determined that the antioxidant property of the newly synthesized compound is of medium level.

Evaluation of Antimicrobial Activity. The antimicrobial effect of the title compound in this study was done according to the MIC method. Considering the study results, it was seen that DMSO used as a control did not have a significant

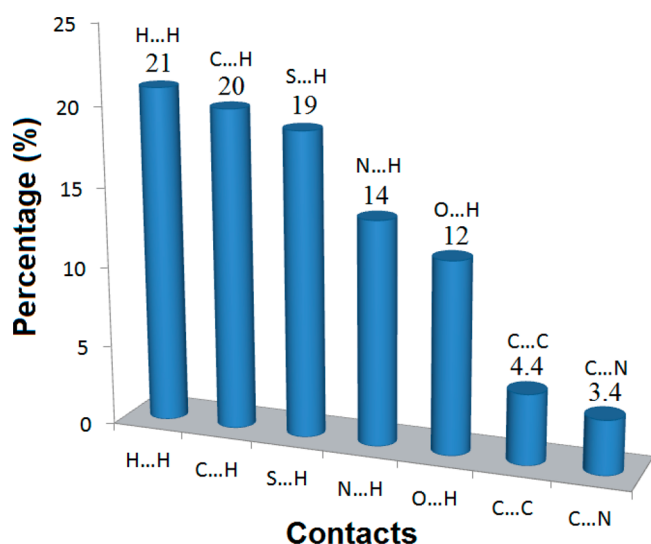


Figure 8. Intermolecular interactions and their percentages in I.

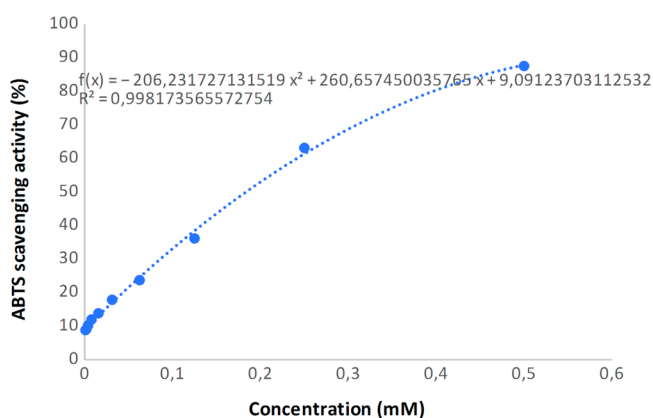


Figure 9. ABTS radical scavenging activity of the title compound.

antimicrobial effect ($>4000 \mu\text{g/mL}$). However, the synthesized title compound has been found to have a significant antimicrobial effect on some microorganisms. When MIC values for gram-negative microorganisms are tested, it is observed that these data are $1000 \mu\text{g/mL}$ for *E. coli* and $2000 \mu\text{g/mL}$ for *S. typhimurium* and *K. pneumoniae*. As shown in Table 2, the MIC values were $250 \mu\text{g/mL}$ for *M. luteus* and *S. aureus*, which are among the gram-positive microorganisms, besides this, the value was $125 \mu\text{g/mL}$ for *L. monocytogenes*. Further to this, the MIC values were determined to be $2000 \mu\text{g/mL}$ for two yeast *Candida* species (i.e., *C. krusei* and *C. glabrata*).

As a result of the study, it is seen that the synthesized substance affects *E. coli* most among gram-negative bacteria. In addition, among gram-positive bacteria, it was determined that it affects *L. monocytogenes* more than others. When gram-positive and gram-negative bacteria were compared, it was tested that it affects gram-positive microorganisms more than gram-negative. It has been determined that it affects the gram-positive *L. monocytogenes* more than any other microorganism.

L. monocytogenes causes meningitis, encephalitis, and septicemia in nonpregnant adults.⁵⁸ It is known that especially elderly people or those who have cellular immunity weakened, such as organ transplantation and lymphoma. It is also an important bacterium in terms of the high mortality rate in the elderly and in immunocompromised patients.⁵⁹ Increasing

resistance to antibiotics in recent years leads people to new alternatives. Therefore, the new chemical synthesized in this study is considered to be important in the fight against such bacteria (especially for *L. monocytogenes*), which are considered to be a risk to human health.

CONCLUSIONS

The studied compound I, $\text{C}_{11}\text{H}_8\text{N}_2\text{OS}_2$, which was synthesized in a two-step procedure, was examined using IR, ^1H NMR, and ^{13}C NMR spectroscopic studies. In this two-step reaction, 2-(thiophen-2-yl)acetic acid was first activated by conversion to 2-(thiophen-2-yl)acetyl chloride and then reacted with 2-aminothiophene-3-carbonitrile. Density functional theory (DFT) at the B3LYP/6-311++G(d,p) level of theory was used to determine the ground-state optimized geometry of I. Appropriate regions for the electrophilic and nucleophilic attack were searched using location-based identifiers in the form of fused Fukui function. The DNA/ECT predicted charge transfer from I to the DNA bases (such as cytosine, adenine, guanine, and thymine). ECT values showed that the molecule can interact more with thymine than with other DNA bases. Also, only the thymine base is treated as an electron acceptor.

ASSOCIATED CONTENT

Supporting Information

The Supporting Information is available free of charge at <https://pubs.acs.org/doi/10.1021/acsomega.2c00318>.

Cif file for compound I (CIF)

CheckCIF/PLATON report (PDF)

AUTHOR INFORMATION

Corresponding Authors

Mohammad Azam – Department of Chemistry, College of Science, King Saud University, Riyadh 11451, Saudi Arabia; orcid.org/0000-0002-4274-2796; Email: azam_res@yahoo.com

Sevgi Kansiz – Department of Fundamental Sciences, Faculty of Engineering, Samsun University, Samsun 55420, Turkey; Email: sevgi.kansiz@samsun.edu.tr

Authors

Şükriye Çakmak – Department of Medical Services and Techniques, Vocational School of Health Services, Sinop University, 57000 Sinop, Turkey; orcid.org/0000-0002-2221-0098

Cem Cüneyt Ersanlı – Department of Physics, Faculty of Arts and Sciences, Sinop University, 5700 Sinop, Turkey

Önder İdil – Department of Basic Education, Faculty of Education, Amasya University, 05000 Amasya, Turkey

Aysel Veyisoğlu – Department of Medical Services and Techniques, Vocational School of Health Services, Sinop University, 57000 Sinop, Turkey

Hasan Yakan – Department of Science and Mathematics Education, Ondokuz Mayıs University, 55139 Samsun, Turkey

Halil Kütük – Department of Chemistry, Faculty of Arts and Sciences, Ondokuz Mayıs University, 55139 Samsun, Turkey

Arunabhram Chutia – School of Chemistry, University of Lincoln, Lincoln LN6 7TS, U.K.; orcid.org/0000-0002-5897-1729

Complete contact information is available at:

https://pubs.acs.org/10.1021/acsomega.2c00318

Notes

The authors declare no competing financial interest.

ACKNOWLEDGMENTS

The authors acknowledge the financial support through Researchers Supporting Project Number (RSP-2021/147), King Saud University, Riyadh, Saudi Arabia. This study was supported by Sinop University as a Scientific Research Project (Project No.: SHMYO-1901-17-25). The authors acknowledge the Scientific and Technological Research Application and Research Center, Sinop University, Turkey, for the use of the Bruker D8 QUEST diffractometer.

REFERENCES

- (1) Chan, W. K.; Ho, C. M.; Wong, M. K.; Che, C. M. Oxidative amide synthesis and N-terminal α -Amino group ligation of peptides in aqueous medium. *J. Am. Chem. Soc.* **2006**, *128*, 14796–14797.
- (2) Gawande, M. B.; Branco, P. S. An efficient and expeditious Fmoc protection of amines and amino acids in aqueous media. *Green Chem.* **2011**, *13*, 3355–3359.
- (3) Humphrey, J. M.; Chamberlin, A. R. Chemical synthesis of natural product peptides: Coupling methods for the incorporation of noncoded amino acids into peptides. *Chem. Rev.* **1997**, *97*, 2243–2266.
- (4) Carey, J. S.; Laffan, D.; Thomson, C.; Williams, M. T. Analysis of the reactions used for the preparation of drug candidate molecules. *Biomol. Chem.* **2006**, *4*, 2337–2347.
- (5) Roughley, S. D.; Jordan, A. M. The medicinal chemist's toolbox: An analysis of reactions used in the pursuit of drug candidates. *J. Med. Chem.* **2011**, *54*, 3451–3479.
- (6) Şener, E. A.; Bingöl, K. K.; Ören, İ.; Arpacı, Ö. T.; Yalçın, İ.; Altanlar, N. Synthesis and microbiological activity of some N-(*o*-hydroxyphenyl)benzamides and phenylacetamides as the possible metabolites of antimicrobial active benzoxazoles: part II. *Il Farmaco* **2000**, *55* (6-7), 469–476.
- (7) Fu, J.; Cheng, K.; Zhang, Z.-M.; Fang, R.-Q.; Zhu, H.-L. Synthesis, structure and structure-activity relationship analysis of caffeic acid amides as potential antimicrobials. *Eur. J. Med. Chem.* **2010**, *45* (6), 2638–2643.
- (8) Carbone, D.; Ebstein, F.; Rabu, C.; Petit, J. Y.; Gregoire, M.; Lang, F. A new carboxamide compound exerts immuno-suppressive activity by inhibiting dendritic cell maturation. *Eur. J. Immunol.* **2005**, *35*, 546–556.
- (9) Kushwaha, N.; Saini, R. K.; Kushwaha, S. K. Synthesis of some amide derivatives and their biological activity. *Int. J. Chem. Technol. Res.* **2011**, *3* (1), 203–209.
- (10) Li, X.; Li, Z.; Deng, H.; Zhou, X. An efficient protocol for the preparation of amides by copper-catalyzed reactions between nitriles and amines in water. *Tetrahedron Lett.* **2013**, *54* (18), 2212–2216.
- (11) Chandra Shekhar, A.; Ravi Kumar, A.; Sathiah, G.; Luke Paul, V.; Sridhar, M.; Shanthan Rao, P. Facile N-formylation of amines using Lewis acids as novel catalysts. *Tetrahedron Lett.* **2009**, *50* (50), 7099–7101.
- (12) Suzuki, K.; Nagasawa, H.; Uto, Y.; Sugimoto, Y.; Noguchi, K.; Wakida, M.; Wierzba, K.; Terada, T.; Asao, T.; Yamada, Y.; et al. Naphthalimidobenzamide DB-51630: A novel DNA binding agent inducing p300 gene expression and exerting a potent anti-cancer activity. *Bioorg. Med. Chem.* **2005**, *13* (12), 4014–4021.
- (13) Yu, B.; Tang, L.; Li, Y.; Song, S.; Ji, X.; Lin, M.; Wu, C.-F. Design, synthesis and evaluation of clinafloxacin triazole hybrids as a new type of antibacterial and antifungal agents. *Bioorg. Med. Chem. Lett.* **2012**, *22* (1), 110–114.
- (14) Karanth, S. N.; Badiadka, N.; Balladka Kunhanna, S.; Shashidhara, K. S.; Peralam Yegneswaran, P. Synthesis of novel Schiff base benzamides via ring opening of thienylidene azlactones for potential antimicrobial activities. *Res. Chem. Intermed.* **2018**, *44*, 4179–4194.
- (15) Rehse, K.; Kotthaus, J.; Khadembashi, L. New 1H-pyrazole-4-carboxamides with antiplatelet activity. *Arch. der Pharm.* **2009**, *342*, 27–33.
- (16) Graul, A.; Castaner, J. Atorvastatin calcium. *Drugs Future.* **1997**, *22*, 956–968.
- (17) Humphrey, J. M.; Chamberlin, A. R. Chemical synthesis of natural product peptides: Coupling methods for the incorporation of noncoded amino acids into peptides. *Chem. Rev.* **1997**, *97* (6), 2243–2266.
- (18) Milenković, D.; Avdović, E.; Dimić, D.; Sudha, S.; Ramarajan, D.; Milanović, Z.; Trifunović, S.; Marković, Z. S. Vibrational and Hirshfeld surface analyses, quantum chemical calculations, and molecular docking studies of coumarin derivative 3-(1-m-toluidinoethylidene)-chromane-2,4-dione and its corresponding palladium(II) complex. *J. Mol. Struct.* **2020**, *1209*, 127935.
- (19) Milenković, D.; Dimitrić Marković, J. M.; Dimić, D.; Jeremić, S.; Amić, D.; Stanojević Pirković, M.; Marković, Z. S. Structural characterization of kaempferol: A spectroscopic and computational study. *Maced. J. Chem. Chem. Eng.* **2019**, *38*, 49–62.
- (20) Cakmak, S.; Kutuk, H.; Odabasoglu, M.; Yakan, H.; Buyukgungor, O. Spectroscopic properties and preparation of some 2,3-dimethoxybenzamide derivatives. *Lett. Org. Chem.* **2016**, *13* (3), 181–194.
- (21) Kırca, B. K.; Çakmak, Ş.; Kütük, H.; Odabaşoğlu, M.; Büyükgüngör, O. Synthesis and characterization of 3-acetoxy-2-methyl-N-(phenyl)benzamide and 3-acetoxy-2-methyl-N-(4-methylphenyl)benzamide. *J. Mol. Struct.* **2018**, *1151*, 191–197.
- (22) APEX2; Bruker AXS Inc.: Madison WI, 2013.
- (23) Sheldrick, G. M. SHELXT-Integrated space-group and crystal-structure determination. *Acta Crystallogr. A: Found. Adv.* **2015**, *71*, 3–8.
- (24) Sheldrick, G. M. Crystal structure refinement with SHELXL. *Acta Crystallogr. C: Struct. Chem.* **2015**, *71*, 3–8.
- (25) Macrae, C. F.; Edgington, P. R.; McCabe, P.; Pidcock, P. E.; Shields, G. P.; Taylor, R.; Towler, M.; van de Streek, J. Mercury: Visualization and analysis of crystal structures. *J. Appl. Crystallogr.* **2006**, *39*, 453–457.
- (26) Spek, A. L. Single-crystal structure validation with the program PLATON. *J. Appl. Crystallogr.* **2003**, *36*, 7–13.
- (27) Farrugia, L. J. WinGX and ORTEP for Windows: an update. *J. Appl. Crystallogr.* **2012**, *45*, 849–854.
- (28) Westrip, S. P. publCIF: Software for editing, validating and formatting crystallographic information files. *J. Appl. Crystallogr.* **2010**, *43*, 920–925.
- (29) Frisch, M. J.; Trucks, G. W.; Schlegel, H. B.; Scuseria, G. E.; Robb, M. A.; Cheeseman, J. R.; Montgomery, J. A., Jr.; Vreven, T.; Kudin, K. N.; Burant, J. C.; Millam, J. M.; Iyengar, S. S.; Tomasi, J.; Barone, V.; Mennucci, B.; Cossi, M.; Scalmani, G.; Rega, N.; Petersson, G. A.; Nakatsuji, H.; Hada, M.; Ehara, M.; Toyota, K.; Fukuda, R.; Hasegawa, J.; Ishida, M.; Nakajima, T.; Honda, Y.; Kitao, O.; Nakai, H.; Klene, M.; Li, X.; Knox, J. E.; Hratchian, H. P.; Cross, J. B.; Bakken, V.; Adamo, C.; Jaramillo, J.; Gomperts, R.; Stratmann, R. E.; Yazyev, O.; Austin, A. J.; Cammi, R.; Pomelli, C.; Ochterski, J. W.; Ayala, P. Y.; Morokuma, K.; Voth, G. A.; Salvador, P.; Dannenberg, J. J.; Zakrzewski, V. G.; Dapprich, S.; Daniels, A. D.; Strain, M. C.; Farkas, O.; Malick, D. K.; Rabuck, A. D.; Raghavachari, K.; Foresman, J. B.; Ortiz, J. V.; Cui, Q.; Baboul, A. G.; Clifford, S.; Cioslowski, J.; Stefanov, B. B.; Liu, G.; Liashenko, A.; Piskorz, P.; Komaromi, I.; Martin, R. L.; Fox, D. J.; Keith, T.; Al-Laham, M. A.; Peng, C. Y.; Nanayakkara, A.; Challacombe, M.; Gill, P. M. W.; Johnson, B.; Chen, W.; Wong, M. W.; Gonzalez, C.; Pople, J. A. *Gaussian 03*, Rev. E.01; Gaussian, Inc., Wallingford, CT, 2004.
- (30) Becke, A. D. Density-functional thermochemistry. III. The role of exact exchange. *J. Chem. Phys.* **1993**, *98*, S648–S652.
- (31) Lee, C.; Yang, W.; Parr, R. G. Development of the Colle-Salvetti correlation-energy formula into a functional of the electron density. *Phys. Rev. B* **1988**, *37*, 785–789.

- (32) Turner, M. J.; MacKinnon, J. J.; Wolff, S. K.; Grimwood, D. J.; Spackman, P. R.; Jayatilaka, D.; Spackman, M. A. *Crystal Explorer*, Ver. 17.5; University of Western Australia: 2017. <https://wiki.crystalexplorer.net/features/hirshfeldsurface>.
- (33) Hasan Tanak; Karataş, Ş.; Meral, S.; Açar, A. A. Crystal structure, spectroscopic and DFT computational studies of N-(4-fluorophenyl)-1-(5-nitrothiophen-2-yl)methanimine. *Crystallogr. Rep.* **2020**, *65* (7), 1221–1225.
- (34) Evecen, M.; Tanak, H.; Açar, A. A.; Meral, S.; Özdemir, N. Comparative structural, spectroscopic and nonlinear optical analysis of a Schiff base compound with experimental and theoretical methods (HF, B3LYP and WB97X-D). *Optik* **2021**, *228*, 166133.
- (35) Hasan Tanak; Karataş, Ş.; Meral, S.; Açar, A. A. Synthesis, molecular structure and quantum chemical studies of N-(2-fluorophenyl)-1-(5-nitrothiophen-2-yl)methanimine. *Crystallogr. Rep.* **2020**, *65* (7), 1212–1216.
- (36) Watanabe, Y.; Mukaiyama, T. A convenient method for the synthesis of carboxamides and peptides by the use of tetrabutylammonium salts. *Chem. Lett.* **1981**, *10* (3), 285–288.
- (37) Hoegberg, T.; Stroem, P.; Ebner, M.; Raemby, S. Cyanide as an efficient and mild catalyst in the aminolysis of esters. *J. Org. Chem.* **1987**, *52* (10), 2033–2036.
- (38) Barrett, A. G.; Lana, J. C. A. Photoluminescence from copper(I) complexes with low-lying metal-to-ligand charge transfer excited states. *J. Chem. Soc. Chem. Commun.* **1978**, *11*, 471–472.
- (39) Cakmak, S.; Kutuk, H.; Odabasoglu, M.; Yakan, H.; Buyukgungor, O. Spectroscopic properties and preparation of some 2,3-dimethoxybenzamide derivatives. *Lett. Org. Chem.* **2016**, *13* (3), 181–194.
- (40) Demir, S.; Cakmak, S.; Dege, N.; Kutuk, H.; Odabasoglu, M.; Kepekci, R. A. A novel 3-acetoxy-2-methyl-N-(4-methoxyphenyl)-benzamide: Molecular structural describe, antioxidant activity with use X-ray diffractions and DFT calculations. *J. Mol. Struct.* **2015**, *1100*, 582–591.
- (41) Iriarte, A. G.; Erben, M. F.; Gholivand, K.; Jios, J. L.; Ulic, S. E.; Della Védova, C. O. [Chloro(difluoroacetyl)phosphoramidic acid dichloride ClF₂CC(O)NHP(O)Cl₂, synthesis, vibrational and NMR spectra and theoretical calculations. *J. Mol. Struct.* **2008**, *886* (1–3), 66–71.
- (42) Kirca, B. K.; Çakmak, Ş.; Kütük, H.; Odabaşoğlu, M.; Büyükgüngör, O. Synthesis and characterization of 3-acetoxy-2-methyl-N-(phenyl)benzamide and 3-acetoxy-2-methyl-N-(4-methylphenyl)benzamide. *J. Mol. Struct.* **2018**, *1151*, 191–197.
- (43) Demircioğlu, Z.; Kaştaş, Ç. A.; Kaştaş, G.; Ersanlı, C. C. Synthesis, crystal structure, computational chemistry studies and Hirshfeld surface analysis of two Schiff bases, (E)-2-[(4-bromo-2-methylphenylimino)methyl]-4-methylphenol and (E)-2-[(4-bromo-2-methylphenylimino)methyl]-6-methylphenol. *Mol. Cryst. Liq. Cryst.* **2021**, *723* (1), 45–61.
- (44) Demircioğlu, Z. Synthesis, crystal structure, spectroscopic characterization, chemical activity and molecular docking studies of (E)-2-(((3-chloro-4-methylphenyl)imino)methyl)-6-ethoxyphenol. *J. Mol. Struct.* **2021**, *1246*, 131114.
- (45) Ayers, P. W.; Parr, R. G. Variational principles for describing chemical reactions: The Fukui function and chemical hardness revisited. *J. Am. Chem. Soc.* **2000**, *122* (9), 2010–2018.
- (46) Parr, R. G.; Szentpály, L. v.; Liu, S. Electrophilicity index. *J. Am. Chem. Soc.* **1999**, *121*, 1922–1924.
- (47) Padmanabhan, J.; Parthasarathi, R.; Subramanian, V.; Chattaraj, P. K. Electrophilicity-based charge transfer descriptor. *J. Phys. Chem. A* **2007**, *111*, 1358–1361.
- (48) McKinnon, J. J.; Jayatilaka, D.; Spackman, M. A. Towards quantitative analysis of intermolecular interactions with Hirshfeld surfaces. *Chem. Commun.* **2007**, 3814–3816.
- (49) Spackman, M. A.; Jayatilaka, D. Hirshfeld surface analysis. *CrystEngComm* **2009**, *11*, 19–32.
- (50) Al-thamili, D. M.; Almansour, A. I.; Arumugam, N.; Kansız, S.; Dege, N.; Soliman, S. M.; Azam, M.; Kumar, R. S. Highly functionalized N-1-(2-pyridinylmethyl)-3,5-bis[(E)-arylmethylidene]-tetrahydro-4(1H)-pyridinones: Synthesis, characterization, crystal structure and DFT studies. *J. Mol. Struct.* **2020**, *1222*, 128940.
- (51) Ramalingam, A.; Kansız, S.; Dege, N.; Sambandam, S. Synthesis, crystal structure, DFT calculations and Hirshfeld surface analysis of 3-chloro-2,6-bis(4-chlorophenyl)-3-methylpiperidin-4-one. *J. Chem. Crystallogr.* **2021**, *51*, 273–287.
- (52) Kansız, S.; Qadir, A.; Dege, N.; Faizi, S. H. Two new copper (II) carboxylate complexes based on N,N,N',N'-tetramethylethylenediamine: Synthesis, crystal structures, spectral properties, dft studies and hirshfeld surface analysis. *J. Mol. Struct.* **2021**, *1230*, 129916.
- (53) Al-Resayes, S. I.; Azam, M.; Trzesowska-Kruszynska, A.; Kruszynski, R.; Soliman, S. M.; Mohapatra, R. K.; Khan, Z. Structural and theoretical investigations, Hirshfeld surface analyses, and cytotoxicity of a naphthalene-based chiral compound. *ACS Omega* **2020**, *5*, 27227–27234.
- (54) Albayati, M. R.; Kansız, S.; Dege, N.; Kaya, S.; Marzouki, R.; Lgaz, H.; Salghi, R.; Ali, I. H.; Alghamdi, M. M.; Chung, I.-M. Synthesis, crystal structure, Hirshfeld surface analysis and DFT calculations of 2-[(2,3-dimethylphenyl)amino]-N'-[(E)-thiophen-2-ylmethylidene]benzohydrazide. *J. Mol. Struct.* **2020**, *1205*, 127654.
- (55) Al-Karawi, A. J. M.; OmarAli, A.-A. B.; Dege, N.; Kansız, S. Formation of a new CuII–triazole ester complex from 1,2-cyclohexanedione-bis(p-bromobenzohydrazone) compound as a consequence of copper(II)-catalyzed click reaction. *Chem. Pap.* **2021**, *75*, 3901–3914.
- (56) Yağcı, N. K.; Kansız, S.; Özçandan, E. Synthesis, crystal structure, DFT studies, Hirshfeld surface analysis and drug delivery performance of bis(2-chloro-4,6-diaminopyrimidine)copper(II)-dichloride. *J. Mol. Struct.* **2021**, *1246*, 131142.
- (57) Halliwell, B. Biochemistry of oxidative stress. *Biochem. Soc. Trans.* **2007**, *35* (5), 1147–1150.
- (58) Murray, P. R.; Baron, E. J.; Jorgensen, J. H.; Landry, M. L.; Pfaller, M. A. *Manual of Clinical Microbiology*, 9th ed.; ASM Press: Washington, DC, 2007, 474–479.
- (59) Evirgen, Ö. Listeria monocytogenes infeksiyonu; kliniği, tanı ve tedavi özellikleri. *Van Tıp Dergisi* **2005**, *12* (1), 32–35.